PERIODICA POLYTECHNICA SER. MECH. ENG. VOL. 44, NO. 1, PP. 171–183 (2000)

THE ROLE OF THE STRESS TRAJECTORIES AS AN AID IN THE CHOICE OF THE SUITABLE SHAPE OF LOAD-BEARING STRUCTURAL ELEMENTS OF ENGINES AND STRUCTURE

Frigyes THAMM

Technical University of Budapest
H–1521 Budapest, Hungary

Received: June 30, 1999

Abstract

The design work on structures and engines begins with the assumption of the shape and dimensions of the parts of them. At this level the designer has nearly total freedom of choice but his skill in the assumption of the layout of the planned item may influence the time and cost necessary to obtain the final product. His choice may be supported effectively by the observation of patterns of stress trajectories taken from different specimens already investigated. Some typical examples of patterns of stress trajectories are collected in this paper together with the explanation of the consequences drawn from them.

Keywords: design aid, stress trajectories.

1. Introduction

In the initial phase of design work the designer has practically total freedom in the choice of the shape of a structural element. As the shape of it does not exist then, no initial strength calculations can be made. Shape and dimensions have to be chosen on the basis of analogy and personal experience. Strength problems have to be treated in subsequent steps of design work, but the cost and duration of the further progress depend strongly on the skill and luck experienced in assuming the general shape of the part in question.

Thus, the designer has to rely in this initial phase to a great part on his 'feelings' based on visual reminiscences. An attempt to collect some experiences into rules may strongly differ from the principles of mechanics as taught in the courses of high schools. As an example for this the booklet of S. UTHE and H. BEHRENT [1] may be mentioned. The authors try to collect their experiences gained in stress research laboratories of the German automotive industry. Their governing idea is that the stresses traverse through a particular part along a 'force path' from the transmission area of the active loads along the stiffest parts of it to the supports along the shortest possible way between both. As the stress distribution is continuous in the whole part, the lateral dimensions of this 'path' cannot be stated accurately. Any arbitrary assumption of it would surely omit some proportion of the transmitted load. This proportion may cause additional stress peaks at the boundary of the part outside the assumed force path. The region of such secondary stress peaks is called by the

authors as the 'boundary stress field'. From the figures presented by the authors it seems that they try to separate the 'force paths' from the remaining part of the specimen by ribbons between the stress trajectories of the stress field. As only some rough sketches about the trajectories are presented by them an attempt was made to collect some trajectory patterns actually derived from calculations or measurements and draw some conclusions from their visual appearance.

2. Some Properties of Stress Trajectories

Stress trajectories are lines in a stress field whose tangents are principal directions of the state of stress. In case of a three-dimensional stress field three mutually perpendicular sets of trajectories exist, forming a three dimensional network. As it is difficult to obtain an impression of such a set, only the two dimensional case of a plane stress field should be investigated now. If in case of a plane stress field for instance in the $x - y$ plane the functions

$$\begin{aligned} \sigma_x &= \sigma_x(x; y), \\ \sigma_y &= \sigma_y(x; y), \\ \tau_{xy} &= \tau_{xy}(x; y), \end{aligned}$$

are known along the whole area of the system, the angle φ of the direction of the principal stresses are defined by the well known formula with the notations of *Fig. 1*:

$$\operatorname{tg} 2\varphi = \frac{2 \operatorname{tg} \varphi}{1 - \operatorname{tg}^2 \varphi} = \frac{2\tau_{xy}}{\sigma_x - \sigma_y} = A(x; y). \tag{1}$$

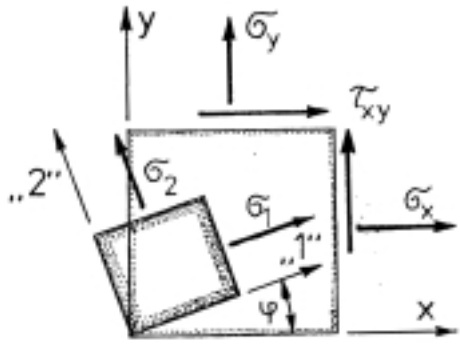

Fig. 1. The notations used for the stress state in a rectangular body element

Resolved to tg φ we obtain the differential equation of the trajectories:

$$\operatorname{tg} \varphi = \frac{\mathrm{d}y}{\mathrm{d}x} = -\frac{1}{A} \pm \sqrt{\frac{1}{A^2} + 1} = -\frac{\sigma_x - \sigma_y}{2\tau_{xy}} \pm \frac{1}{\tau_{xy}} \sqrt{(\sigma_x - \sigma_y)^2 + 4\tau_{xy}^2}. \tag{2}$$

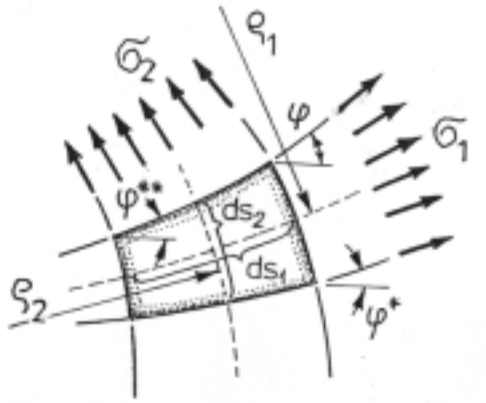

Fig. 2. Stresses in a body element in natural coordinates

The two signs ahead the square root express the mutually perpendicular set of trajectories. Boundary values are the stress components at arbitrary points of the boundary thus producing the complete set of trajectories. At points with $\sigma_x = \sigma_y$ both terms of *Eq.* (2) become indefinite. These points are called as singularities.

Another property of the stress trajectories can be recognized by applying the Lamé–Maxwell equilibrium equations in which the stress trajectories represent a natural coordinate system. Using the notations of *Fig. 2* the equation along the arc length s_1 of the trajectory of σ_1 can be written as

$$-\frac{\partial \sigma_1}{\partial s_1} = -\frac{\sigma_1 - \sigma_2}{\rho_2} = -(\sigma_1 - \sigma_2)\frac{\partial \varphi}{\partial s_2}, \tag{3.a}$$

and similarly for the trajectory of σ_2:

$$\frac{\partial \sigma_2}{\partial s_2} = -\frac{\sigma_1 - \sigma_2}{\rho_1} = -(\sigma_1 - \sigma_2)\frac{\partial \varphi}{\partial s_1}. \tag{3.b}$$

With $\partial\varphi \approx \varphi - \varphi^* \approx \varphi - \varphi^{**}$.

That means that the value of σ_1 or σ_2 increases, when the neighbouring trajectories of the respective principal stress are approaching to each other, that means that the bandwidth between the two trajectories decreases. On the other hand, $\partial\sigma_2/\partial s_2$ resp. $\partial\sigma_1/\partial s_1$ becomes infinite, if the radius ρ_1 resp. ρ_2 becomes zero. This is the case at inner corners of the circumference of the specimen investigated.

As the value of all the stress components in *Eq.* (2) varies from point to point, the analytical solution of *Eq.* (2) is practically impossible except in some extremely simple cases. Numerical solution may be possible but its accuracy largely depends on the element mesh particularly around the singularities. Besides, the treatment

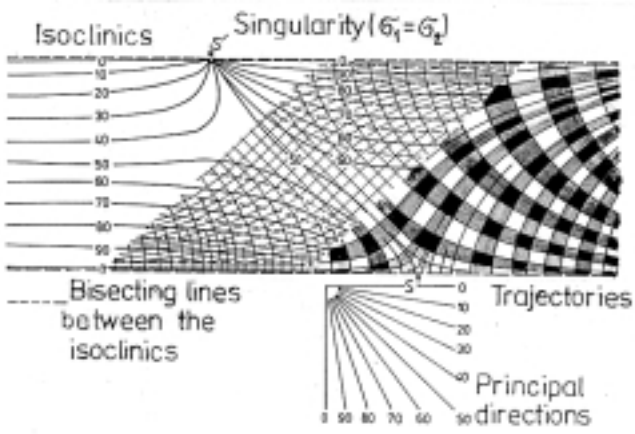

Fig. 3. Drawing the stress trajectories from an isoclinic pattern of plane photoelasticity

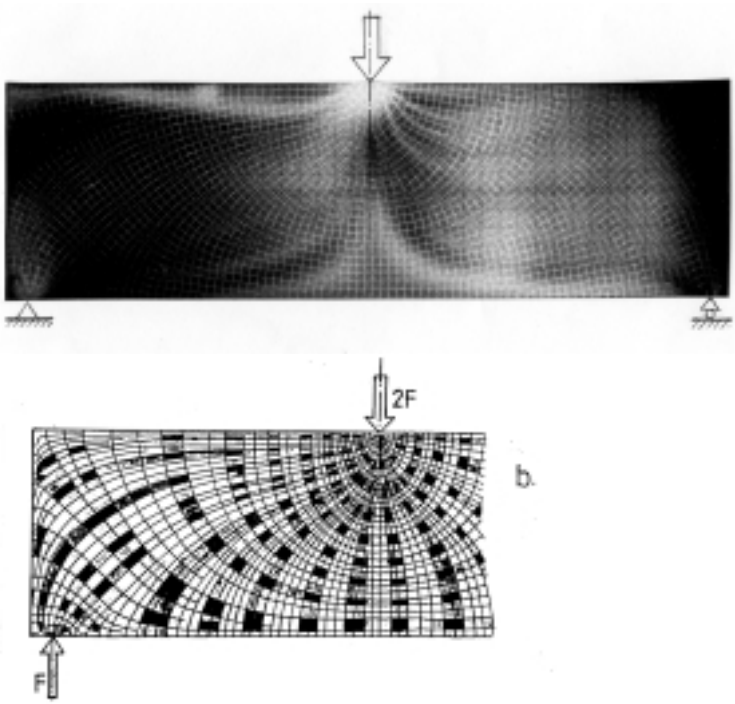

Fig. 4. Pattern of stress trajectories of a short beam in bending. a. derived optically, b. drawn by hand

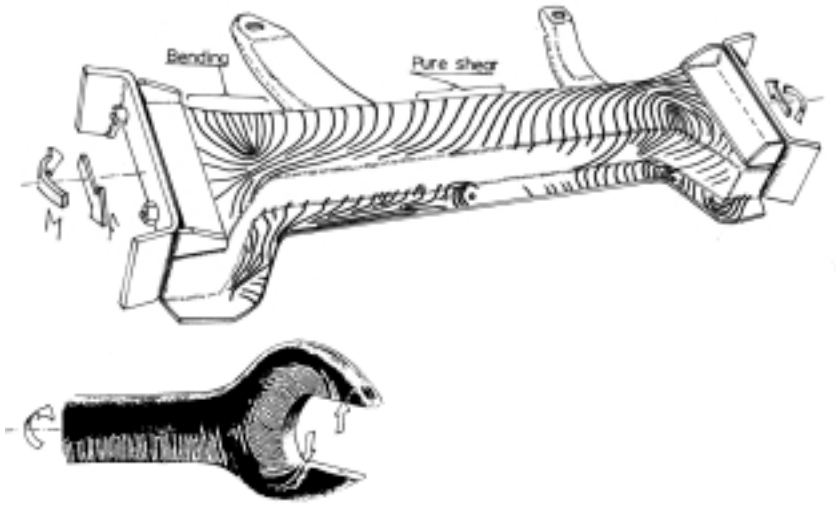

Fig. 5. Crack patterns of stresscoat producing a pattern of the stress trajectories perpendicular to the positive principal stress. a. cross-tie of a vehicle undercarriage. b. a wrench

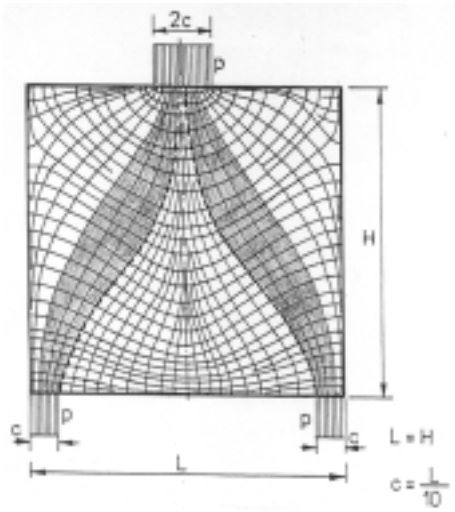

Fig. 6. Theoretically derived pattern of stress trajectories in a square plate. From [5].

of the singularities would present additional problems. This may be the reason that only very few trajectory patterns obtained by numerical calculation are known.

There are two ways to produce stress trajectories experimentally:

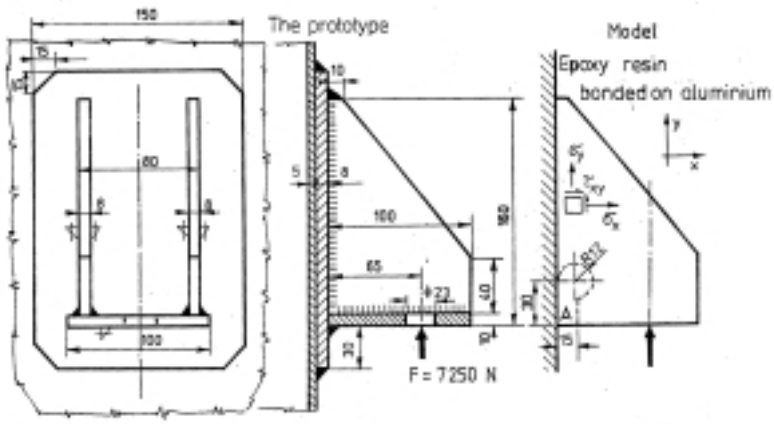

Fig. 7. Prototype and photoelastic model of a tank support

a./ drawing them based on the isoclinic pattern of plane photoelasticity.
b./ applying brittle lacquer on the surface of the specimen investigated.

The isoclinics are lines along which the principal stresses are parallel and can be obtained from photoelastic patterns taken between crossed polarizers without quarter wave plates [2]. The trajectories are obtained from them by a procedure as shown in *Fig. 3*. Straight lines inclined with the angle belonging to a particular isoclinic are drawn between the bisecting lines to the neighbouring isoclincs. These lines are then continued with the angle of the subsequent isoclinic and so forth (middle part of *Fig. 3*). Smooth curves laid upon this sequence of broken lines (right side of *Fig. 3*) are the trajectories. To enhance the impression of them bands between neighbouring lines were shadowed. This procedure is extremely cumbersome, but there exists a procedure by which the trajectories are produced optically [3] [4]. *Fig. 4* shows at the top the optically obtained trajectories of a short beam on two supports and at the bottom the same set of trajectories produced graphically by hand. The good agreement between both can be clearly seen.

The brittle lacquer painted or sprayed upon the surface of a specimen has the property to crack along lines perpendicular to the positive stress trajectory, when subjected to loads of proper magnitude. Thus parts of the trajectory of the smaller principal stress are produced. The examples of such crack patterns are shown in *Fig. 5*.

3. Examples of Patterns of Stress Trajectories and the Conclusions They Offer

Trajectory pattern of a square plate theoretically derived by [5] is shown in *Fig. 6*. As seen from the pattern most of the trajectories starting from the active load at the

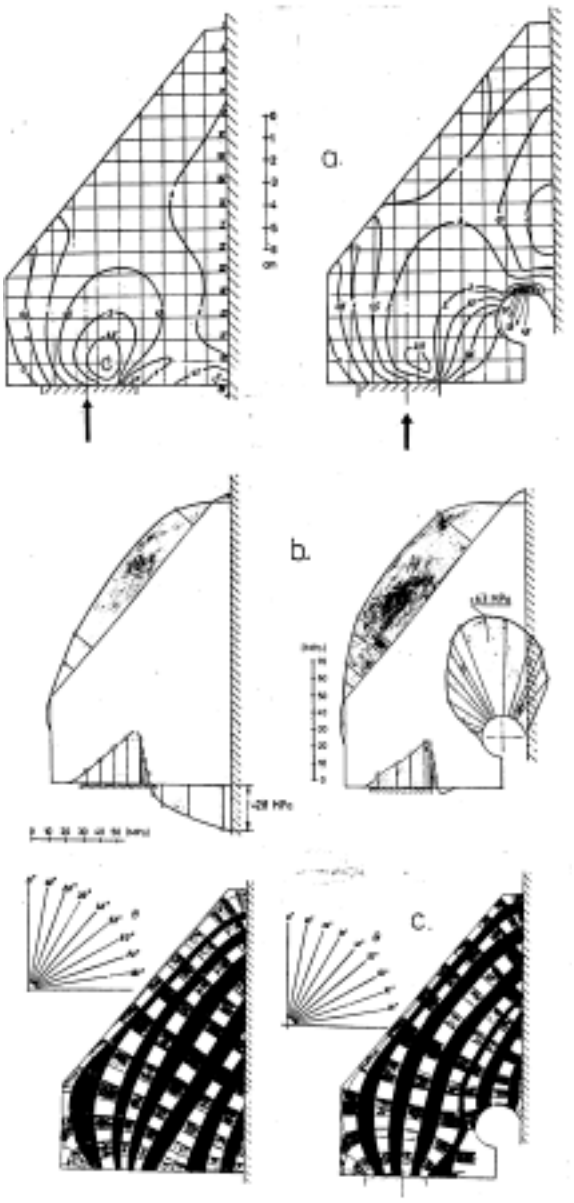

Fig. 8. Results of the photoelastic investigation of the model shown in *Fig. 7.* a. isochromatic fringe pattern. b. boundary stress distribution. c. the set of stress trajectories.

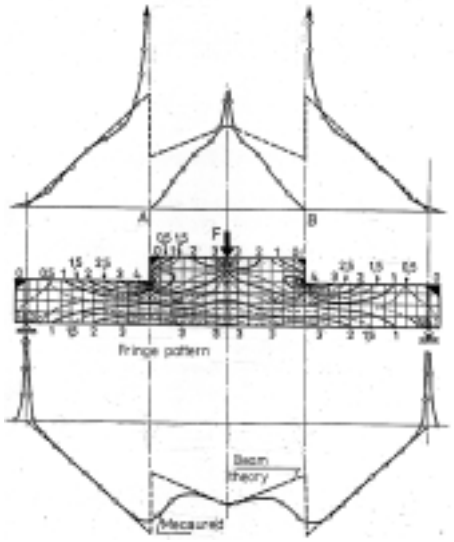

Fig. 9. Isochromatic fringe pattern and boundary stresses of a bent beam with a height step.

center of the upper edge of the plate reach the two reactive loads at the corners of the lower edge. It can be concluded therefore that the other set of trajectories does not represent stresses of important magnitude, in contrast to the pattern shown in *Fig. 4* where most of the trajectories originating from the active force end at the free boundary on the lower edge. Thus high bending stresses appear along the other set of trajectories.

Fig. 7 shows a support on a vertical cylindric tank wall and the model arrangement for its photoelastic investigation. Due to the sharp corner at the lower edge of support (point '*A*') high stress concentration was expected there. Therefore, an attempt was made to create a smooth end of the junction there as shown by the dashed line in the picture of the model. *Fig. 8* shows the set of isochromatic fringes in both cases (part a), the boundary stresses (part b) and the stress trajectories (part c). In contrast to the expectations the altered design showed a considerable increase of the stress peak which can be explained by the fact that the cutout came near to the main trajectory band and caused a curved path of it.

The photoelastic fringe pattern of a beam on two supports with a height step and loaded by a single force at the center of the span is seen in *Fig. 9* including the boundary stress distribution as calculated by the elementary beam theory, compared with measurement results. Considerable deviation between both can be seen in the neighbourhood of the beam height step, the measured values at points *A* and *B* reaching extremely high values of indefinite magnitude. To avoid them a groove at the point of the stress peak was machined into the model as shown in *Fig. 10*. The altered fringe pattern is shown in part a. of the figure; part b. shows the set

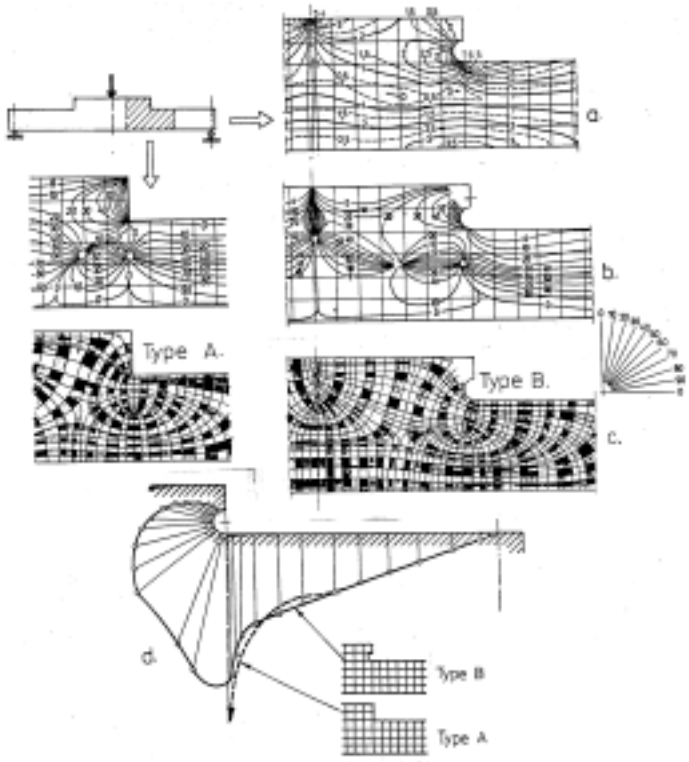

Fig. 10. Comparison of the original stress state of the region of the height step (Type A) with that of the same region but modified by a cutout at the inner corner of the beam (Type B). a. fringe pattern of the modified beam. b. isoclinic pattern. c. stress trajectories. d. comparison of the boundary stresses of the two cases.

of isoclinics and part c. the stress trajectories in both cases. Through the groove the sharp corner of the trajectory was avoided and with it the stress peak lowered in spite of material removal.

The photoelastic examination of a short cantilever clamped by two bolts is shown in *Fig. 11.* Part a. shows the dimensions of the model, part b. the isochromatic fringe pattern and part c. the stress trajectories. Here is a marked difference between the shape of the two sets of trajectories reaching the bolts. The going around the upper bolt is that of the bigger tensile principal stress. The lower bolt directly attracts the trajectories of the compressive lower principal stress causing a single stress peak in the cross section $A - B$ (part d.) in contrast to the other set resulting in two smaller stress peaks.

At beam-like structures stress trajectories inclined by about 45° mean dominant shear. This is seen by a plate with four cutouts loaded in the centre of the

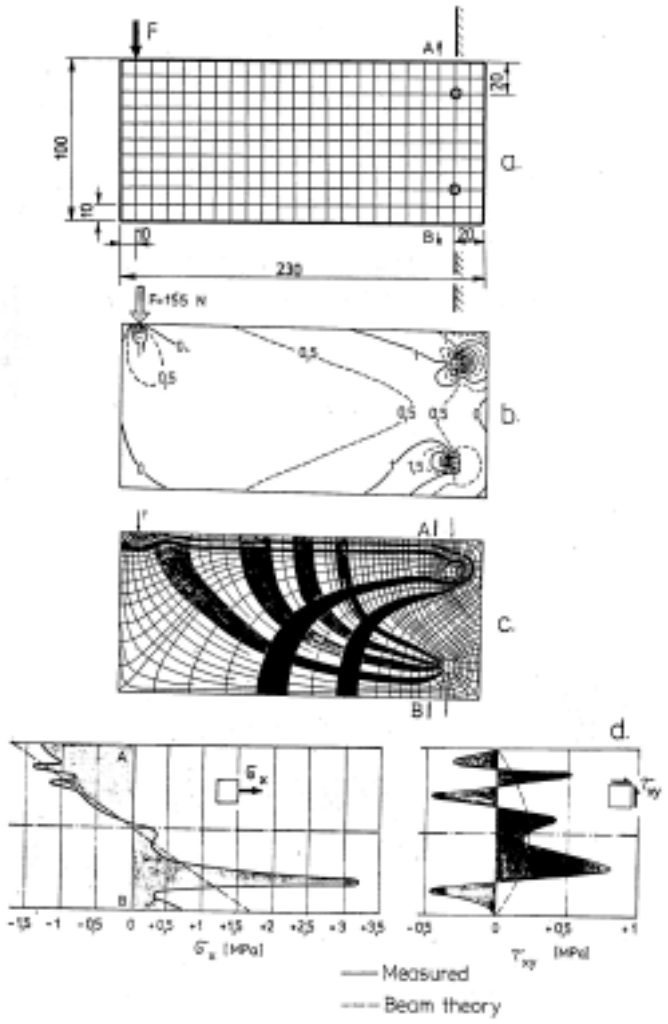

Fig. 11. Photoelastic investigation of a cantilever bar clamped by two bolts. a. dimensions of the model. b. fringe pattern. c. stress trajectories. d. distribution of the longitudinal stress component σ_x and the shear stress τ_{xy} along the line $A - B$ immediately before the cross section of the bolts.

span (*Fig. 12*). As it is seen from the patterns of stress trajectories the central column between the inner cutouts is loaded by practically pure compression where the two others are subjected to practically pure shear. The small arrows pointing upon the boundary of the specimen mark singular points at which the boundary stress changes sign. A similar effect can be observed at part a. of *Fig. 5*.

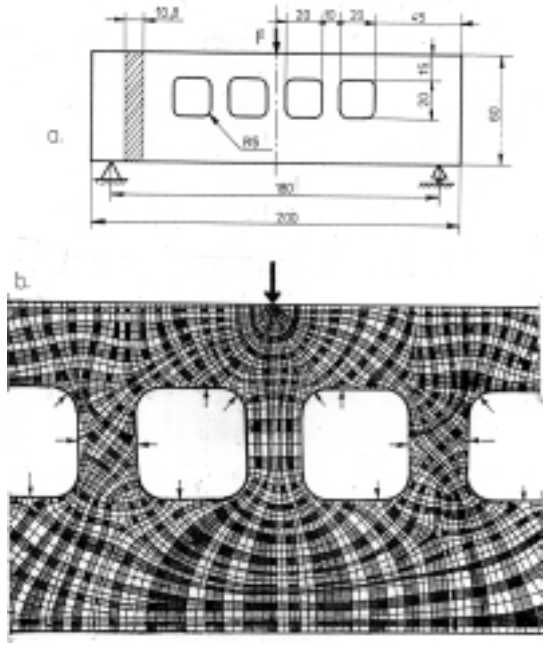

Fig. 12. Photoelastic investigation of a high bar in bending with cutouts. a. dimensions and loading of the model. b. stress trajectories in the middle part of the model.

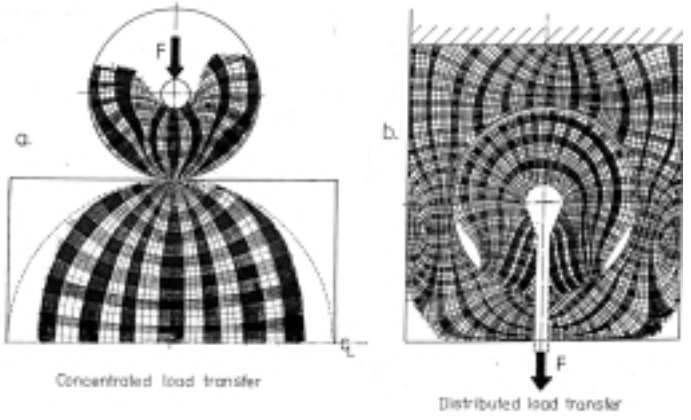

Fig. 13. Stress trajectories in regions of force transfer. a. load transfer from a roller to a square plate. b. nut and bolt connection with small clearance between both.

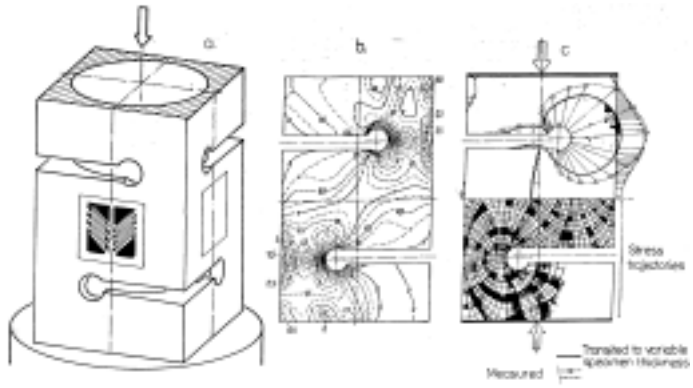

Fig. 14. Photoelastic investigation of the stress distribution in the strain gage operated load cell of a force transducer. a. the shape of the load cell with the position of the strain gages. b. isochromatic fringe pattern taken from a plane model of one side of the cell. c. upper part: boundary stress distribution and shear stress at the location of the gages. lower part: stress trajectories showing their 45°-inclination at the location of the strain gages.

Stress trajectories around regions of load transfer are shown in *Fig. 13.* At left (part a.) the load is transmitted concentrated on a square plate (only the upper part of it is shown). Practically, all trajectories run between the two points of load transfer and therefore the other set of nearly horizontal trajectories represent only negligible magnitude of stress. The roller also contains trajectories traversing from the point of contact to the plate to the loading bolt but there are also trajectories which tend to travel around the bolt. They can be seen only on the side of the roller because they tend to diminish at the upper side of the roller. This set of trajectories is originated by the influence of Poisson's ratio upon the stress distribution.

Fig. 14 shows patterns obtained from a photoelastic investigation of the load cell of a force transducer. Part a. shows the load cell itself with the location of the shear strain gages. Isochromatic fringe pattern taken from a plane photoelastic model is seen on part b. revealing high stress concentration at the roots of the grooves machined into the block of the load cell body to create approximately pure shear along the strain gages. The measured values are transited to the actual prototype of variable thickness by the method of HEYMANN [6]. The boundary stresses are shown on the upper part of c. of *Fig. 14*, the stress trajectories at the bottom of the same figure. They reveal the desired inclination by 45° at the loci of the strain gages, but also indicate the high stresses at the root of the grooves as already mentioned. They are due to the sharp curvature of the trajectories and their maximum value is much higher than that at the strain gages. As similar stress peaks are found in the load cells of force transducers of different kinds, this indicates the necessity of the choice of high strength steel for the transducer body in order to

obtain the necessary accuracy and linearity of the whole transducer.

4. Conclusions

Though the stress trajectories do not present the magnitude of stresses their appearance may lead to better understanding of the nature of stress fields. Observing and comparing trajectory patterns as having been shown in the presented examples may give to the designer the feeling of soundness in the choice of the shape of the parts he wants to apply especially in the initial phase of design.

References

[1] UTHE, S. – BEHRENT, H.: Von der Spannungsanalyse zum betriebsfesten Bauteil. Edition of the authors.
[2] FROCHT, M. M.: Photoelasticity. John Wiley and Sons. 1944–48.
[3] VASÁRHELYI, D.: Contribution to the Calculation of Stress from Photoelastic Values, *Am. Soc. Exp. Stress. Anal.*, 1951.
[4] THAMM, F. – ÁGOSTON, GY.: Aufbau, Arbeitsweise und Fehlerquellen des Trajektorienzeichners für spannungsoptische Isoklinenaufnahmen. *Z. f. Instrumentenkunde* Vol. 72 (1964) pp. 63–71.
[5] PFEIFFER, G.: Berechnung und Bemessung von wandartigen Trägern. Werner-Verlag, Düsseldorf, 1968.
[6] HEYMANN, J.: Experimentelle Untersuchungen eines Profil-ebenen Spannungszustandes. *Proc. 4th Int. Conf. on Experimental Stress Analysis*, Cambridge 1970, pp. 505–512.